Nozzle Characteristics in the Transition Regime between Continuum and Free Molecular Flow

MANCIL W MILLIGAN*
University of Tennessee, Knoxville, Tenn

Experimental measurements were made of the flow characteristics of a convergent-divergent nozzle, two convergent nozzles, and an orifice Data were obtained on the variations of the mass flow rate of argon with pressure ratio across the test specimens and the variations of discharge coefficient with Reynolds number and Knudsen number The results are partially explained, and, in view of the scarcity of experimental data in this transition regime between continuum and free molecular flow, they should be of value to fluid dynamicists who are attempting to design in this flow regime and to those individuals who are attempting to theoretically analyze this flow regime

Nomenclature

A = area of physical throat
C_d = discharge coefficient; ratio of the actual mass flow to the ideal one-dimensional isentropic mass flow
d = equivalent diameter of molecule
K = Boltzmann constant
L = axial length of test section
$\dot{m}_a$ = actual mass flow
$\dot{m}_t$ = theoretical one-dimensional isentropic mass flow
$\dot{n}$ = molecule flow rate
M = molecular weight
N_{Ku} = Knudsen number
N_M = Mach number
N_{Re} = Reynolds number
P = absolute pressure
$\dot{P}$ = pressure change per unit time
r = radius of flow passage
R = universal gas constant
T = absolute temperature
V = volume of stagnation tank
Z = molecule flow parameter
γ = ratio of specific heats
η = absolute viscosity
λ = mean free path
ρ = density
$\mathfrak{M}$ = mass per molecule

Subscripts

1 = station upstream of nozzle or orifice (stagnation tank)
2 = physical throat of nozzle or orifice
3 = station downstream of nozzle or orifice (downstream tank)

Introduction

RECENTLY the interest in nozzle flow at low densities has been greatly increased because of the demands of current technology for very low-density gas streams and the need of devices to be used as flowmeters for low-density gas streams The designer of nozzles to operate at very low densities is faced with the problem of determining dimensions that will permit the nozzle to operate at the desired conditions Smetana[1] has pointed out that the problem lies in the calculation of the boundary-layer displacement thickness At normal densities, this is fairly straightforward; but at low densities, the procedure is more involved, since the boundary layer is quite thick and tends to fill the entire nozzle as the density is reduced In addition to the problem of determining displacement thickness in order to compensate for boundary-layer flow, there is the additional complication of compensating for the slip at the solid boundaries at low densities

In the past, very little experimental information has been made available which could be used to guide and support a theoretical description of the flow through nozzles in the transition regime between continuum and free molecular flow Folsom[2] reported experimental data on two types of convergent nozzles at low densities but gave little analysis of the data Liepmann[3] has reported results on flow through orifices at low densities, but his results are not directly applicable to nozzle flow Recently, Smetana[4] has presented significant data for nozzle flow at low densities His results are primarily in the form of discharge coefficients as a function of Reynolds number or upstream pressure Smetana attempted to correlate his results with that of earlier investigators Apparently none of these investigators has given attention to the variation of nozzle characteristics with Knudsen number In effect, most of the previous experimental studies have been directed to the viscous aspects of this flow regime without due consideration of the slip velocity at the solid boundaries

Results are included here for one converging-diverging nozzle, two converging nozzles, and one orifice These results have proved to be quite informative insofar as providing qualitative explanation of the flow phenomena in the transition regime

Experimental Procedure

In order to determine the mass flow rate through the different flow passages, a quasi-steady-flow technique was used Upstream of the nozzle or orifice under investigation (hereafter referred to as the test section) a rigid tank served as a stagnation reservoir The volume of this tank was carefully determined by measurement A quick acting flow control valve was located between this upstream tank and the test section The ideal gas equation of state was used to determine the number of molecules which left the stagnation tank in a measured time interval This was accomplished by applying the ideal gas equation of state before and after the time interval of flow Both pressure and temperature were measured in the stagnation tank Downstream of the test section another rigid tank served as downstream sink for the flow This downstream tank was connected to a pumping system capable of maintaining the desired densities and flow

Received December 10, 1963; revision received March 16, 1964 The author wishes to thank Harvey J Wilkerson for his assistance in setting up much of the experimental apparatus and in conducting many of the early tests

* Assistant Professor, Department of Mechanical and Aerospace Engineering Member AIAA

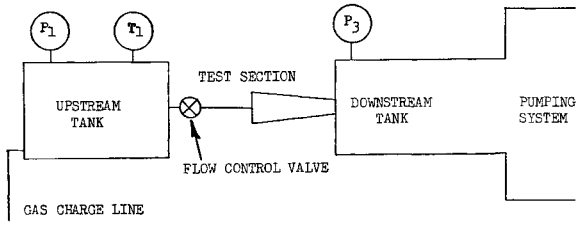

Fig 1 Experimental facility

rates Figure 1 is a schematic diagram of the experimental facility

The volume of the stagnation reservoir (upstream tank) was 0 843 ft^3, and the volume of the downstream tank was approximately 4 times that of the upstream tank The time interval was chosen such that the pressure in the stagnation reservoir P_1 changed less than 10% during the measured time interval Using this procedure, $\dot{P}_1$ was approximately constant for any one time interval All pressures were measured by using McLeod gages

Temperature instrumentation inside the stagnation tank revealed that the expansion of the gas remaining in the tank was essentially isothermal during these flow intervals, so that the molecular flow rate through the test section could be determined as

$$\dot{n} = -(V/KT)(\dot{P}_1) \tag{1}$$

By using Eq (1), it was possible to obtain molecular flow rates for a known pressure potential across the test section By varying the stagnation pressure P_1 and the downstream pressure P_3, it was possible to obtain data on the variation of mass rate with pressure ratio across the test section and the degree of rarefication This experimental technique was verified by using a long tube as a test section Brown,[5] Weber,[6] and many others have shown a very good agreement between experimental data and theoretically predicted values for the long tube The experimental results for flow through a stainless-steel tube with a diameter of 0 269 in and length-to-radius ratio of 336 agreed very well with the predicted values, and this gave a high confidence level to the experimental procedure used to study the nozzles and orifice

Flow Configurations

Four flow passages were investigated in addition to the long tube verification study as just mentioned A detailed description of each flow configuration (test section) is given below All test sections were machined from stainless steel The distance between the stagnation reservoir and the test section was approximately 7 in for all configurations This included the valve, pipe, and union; and the entire length had a flow passage diameter of 0 269 in The test section in each case was mated directly to the downstream tank

Nozzle A: This test section consisted of an entrance cone and an exit cone The entrance cone has an inlet diameter of 0 269 in with an axial length of 0 15 in , and the exit cone had an exit diameter of 0 269 in with an axial length of 0 45 in The two cones intersected at a throat of zero axial length having a diameter of 0 128 in

Nozzle B: This test section consisted of an entrance cone with an inlet diameter of 0 269 in and a throat diameter of 0 129 in The axial length was 0 9 in

Nozzle C: This test section was identical to Nozzle B except that the throat diameter was 0 065 in

Orifice: This test section consisted of a sharp edge orifice with an orifice diameter of 0 128 in The diameter upstream and downstream of the orifice plate was 0 269 in The total axial length was 0 60 in , and the axial length of the orifice plate was 0 04 in

Results

The data obtained for these four test sections were in the form of mass flow rate as a function of pressure potential across the test section For each configuration, data to determine mass rate vs pressure ratio were obtained at three stagnation pressure levels This was done in order to study the effect of rarefication upon the flow The data are presented in the form of Z vs P_3/P_1 plots where

$$Z = \dot{n}(T_1)^{1/2}/A_2P_1 \tag{2}$$

The molecule flow parameter Z was used in order to make the data applicable to conditions at different pressure, temperature, and flow area levels By using this parameter, the molecule flow rate per unit area for flow with different stagnation pressures and temperatures could be related and compared Note that the molecule flow rate can be multiplied by $\mathfrak{M}$ (1 459 $\times$ 10^{-25} lbm/molecule for argon), the mass per molecule, to obtain mass flow rate Figures 2–4 are plots of Z vs P_3/P_1 for the four configurations On Fig 2 the data for nozzle A and B are both presented since nozzle B was used simply to verify the fact that the convergent-divergent nozzle A was, indeed, behaving as a converging nozzle with little or no pressure recovery in the diverging portion Data are plotted for three different levels of rarefication Also shown on these figures are the results of a one-dimensional isentropic analysis for a converging nozzle On Fig 3, the free-molecule flow rate through nozzle C, as predicted by using the results of Sparrow and Jonsson,[7] is shown

In order to obtain additional information from the data, a discharge coefficient was defined as the ratio of the actual mass rate to the one-dimensional theoretical value It is apparent that this discharge coefficient can be written as

$$C_d = \frac{\dot{m}_a}{\dot{m}_T} = \frac{\dot{n}_a}{\dot{n}_T} = \frac{\dot{n}(T_1)^{1/2}/A_2P_1]_{\text{actual}}}{\dot{n}(T_1)^{1/2}/A_2P_1]_{\text{th or}}} \tag{3}$$

This parameter was determined for all configurations at pressure ratios equal to or less than the theoretical critical value ($P_3/P_1 \leqslant 0\,486$) In Figs 5–7, C_d is plotted as a function of Reynolds number where the Reynolds number was

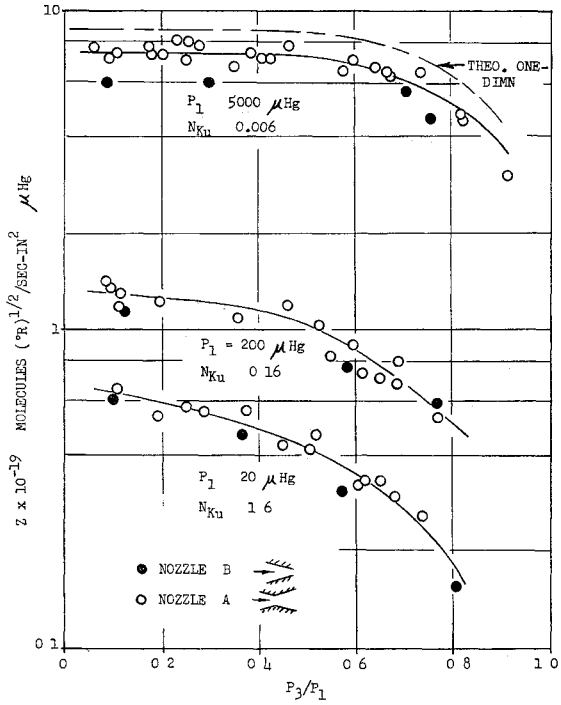

Fig 2 Flow parameter Z vs pressure ratio for nozzles A and B

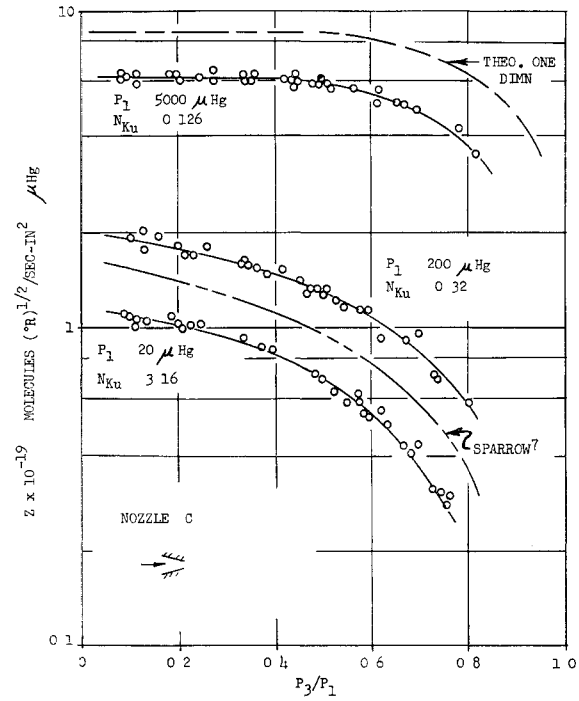

Fig 3 Flow parameter Z vs pressure ratio for nozzle C

defined as

$$N_{Re} = \dot{m}_a r_2 / A_2 \eta_1 \tag{4}$$

Again the results for nozzles A and B are combined on the same plot In Figs 8–10, C_d is plotted as a function of the inverse Knudsen number for the four configurations The Knudsen number was defined as

$$N_{Ku} = \frac{\lambda_1}{r_2} = \frac{KT_1}{2^{1/2} P_1 \pi d^2 r_2} \tag{5}$$

The viscosity and mean free path were evaluated at the upstream section because the temperature and pressure could

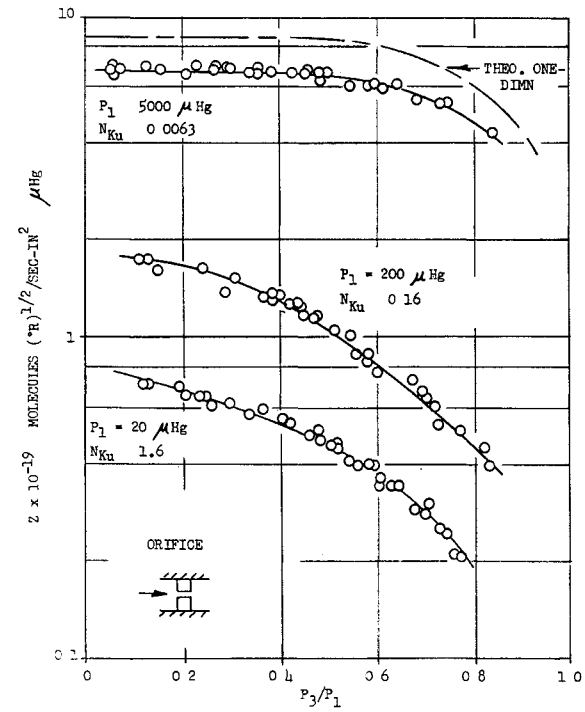

Fig 4 Flow parameter Z vs pressure ratio for orifice

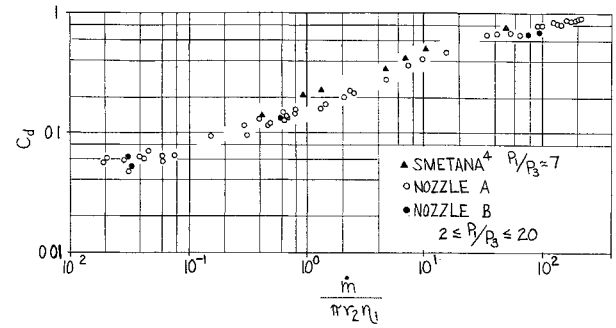

Fig 5 Discharge coefficient vs Reynolds number for nozzles A and B

be reliably measured at station 1 and could not be evaluated at station 2 It is customary to define the Knudsen number in terms of Mach number and Reynolds number for continuum flows Since both of these parameters are basically continuum concepts, it appears desirable to define the Knudsen number in terms of its fundamental meaning [Eq (5)] for low-density flows

Discussion and Conclusions

One of the established facts of continuum gas flow through a nozzle at high Reynolds number is that, when the expansion from the stagnation conditions results in a sonic velocity ($N_{M2} = 1$) at the throat, no additional increase in mass flow rate can be accomplished by decreasing the back pressure This fact is clearly shown in Figs 2 and 3 by the data at the highest stagnation pressures (lowest Knudsen numbers) It is also apparent from these same data that the idealized one-dimensional treatment correctly predicts the character of this flow The remaining data shown on these figures do not exhibit this so-called "choking" phenomenon In fact, as the degree of rarefication increases (lower stagnation pressures and higher Knudsen numbers), the tendency toward a constant mass flow rate is decreased as indicated by the increased slope of the curves through the data points This is explained at least qualitatively by the fact that, as the degree of rarefication increases, more of the nozzle throat is filled with boundary layer consisting of velocities less than sonic, and the molecular diffusion becomes more significant

Since nozzle C had a throat diameter of one-half that of nozzles A and B, the Knudsen number for the smaller nozzle was twice that of the larger ones at identical thermodynamic states of the gas The lowest stagnation pressure for all three of these configurations was approximately 20 μ Hg which corresponds to approximate Knudsen numbers of 1 5 for nozzles A and B and 3 0 for nozzle C From the data shown in Figs 2 and 3 for the 20-μ-Hg stagnation pressure, it was determined that the mass flow rate per unit area at a Knudsen number of 3 0 was approximately 65% greater than at a Knudsen number of 1 5 The results for a long

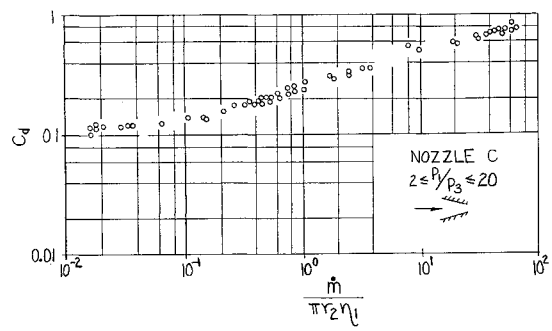

Fig 6 Discharge coefficient vs Reynolds number for nozzle C

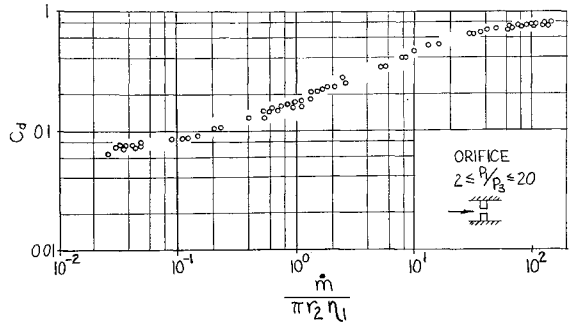

Fig 7 Discharge coefficient vs Reynolds number for orifice

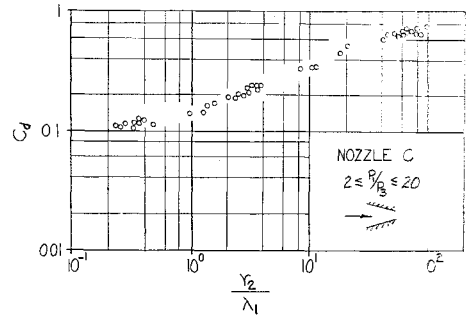

Fig 9 Discharge coefficient vs inverse Knudsen number for nozzle C

tube, as presented by many investigators, indicate a mass flow rate at a Knudsen number of 3 0, which is approximately 65% greater than predicted by the classical Hagen-Poiseuille continuum analysis This tendency to an increased mass flow rate per unit area for the smaller nozzle is also indicated by the 200-μ-Hg data but is reduced in magnitude as would be expected The data for 5000-μ-Hg stagnation pressure shows a decreased mass flow rate per unit area for the smaller nozzle as would be expected, since a greater portion of the smaller nozzle would be filled with viscous flow and there would be no slip at this high stagnation pressure to offset the viscous effect These data clearly establish the importance of the slip flow regime in the design of nozzle to be used at low densities

A comparison of the data for nozzle C and the predicted free-molecule flow for this configuration, as shown on Fig 3, indicates that the experimental data for the 20-μ-Hg stagnation pressure has the character of free-molecule flow The fact that the experimental results give flow rates less than that predicted is explained in part by the fact that there were approximately 7 in of constant area flow passage between the stagnation reservoir and the nozzle inlet This added resistance to flow can account for the deviation

A comparison of the data for the orifice and nozzles A and B, which all had approximately the same throat diameter, indicates that the mass flow rate for the orifice was slightly less than that of the nozzles at the 5000-μ-Hg stagnation pressure level As the degree of rarefication increased (lower stagnation pressures), there was less difference between the nozzle and orifice data

The data shown in Figs 5–10 indicate some change in the character of the flow at a value for the discharge coefficient between 0 40 and 0 60 This is explained at least qualitatively by assuming that this change in character is caused by the throat becoming completely filled with viscous flow If it is assumed that the throat is completely filled with viscous flow having a parabolic velocity distribution, then it is apparent that the discharge coefficient would be approximately 0 50, since the average velocity is one-half the maximum velocity for this distribution (the average height of a paraboloid of revolution is one-half the maximum height) Thus, it was concluded that the throat of the flow passages was not filled with boundary layer for any conditions that resulted in a discharge coefficient greater than 0 60

The data shown in Fig 6 for the smaller nozzle correspond to flow with twice the value of the Knudsen number of the flow indicated by the data in Fig 5 It is apparent from these data that the discharge coefficient at identical Reynolds numbers is greater for the higher Knudsen number flow Thus, it may be concluded that the slip at the solid boundaries becomes quite important at very low densities The results of Smetana[4] are shown on Figs 5 and 8 There appears to be good agreement between these results and those obtained here even though there was a considerable difference in the actual physical configurations

The data shown in Figs 8 and 9 indicate some change in the character of the flow between Knudsen numbers of 1 and 0 1 Data for the long tube indicated that the effect of slip at the wall began to be significant at a Knudsen number of approximately 0 1 Thus, it was concluded that this change in the character of the flow was due to the effect of slip at the walls The data in these figures also indicate that the transition from continuum to slip flow is smooth and involves the interaction of the two types of flow rather than some abrupt change in the character of the flow

Much work remains before the flow in this transition regime is fully understood, but, as more experimental data become available to guide and support theoretical descriptions, the complete understanding of this flow phenomenon is not far in the future

References

[1] Smetana, F O, "A semiempirical description of the discharge characteristics of the converging section of a low-density hypersonic nozzle," J Aerospace Sci **28**, 988–989 (1961)

[2] Folsom R G, Nozzle characteristics in high vacuum flows-rarefied gas dynamics ' Trans Am Soc Mech Engrs **74**, 915–918 (1952)

[3] Liepmann, H W, ' Gaskinetics and gasdynamics of orifice flow, J Fluid Mech **10**, 65–79 (1961)

[4] Smetana, F O, Convergent-divergent nozzle discharge

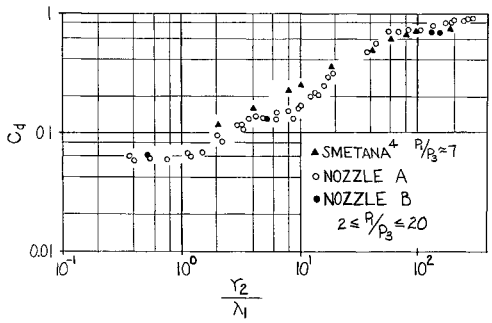

Fig 8 Discharge coefficient vs inverse Knudsen number for nozzles A and B

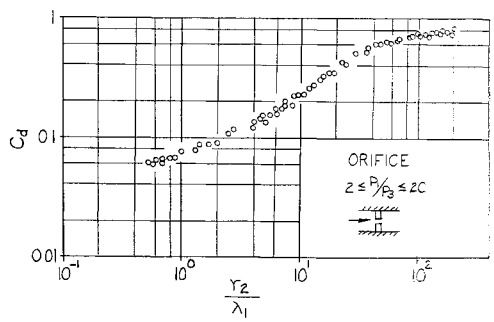

Fig 10 Discharge coefficient vs inverse Knudsen number for orifice

characteristics in the transition regime between free molecule and continuum flow," American Society of Mechanical Engineers Paper 63 WA 94 (1963)

[5] Brown, G P, Di Nardo, A Chevy, G K, and Sherwood, T K, "The flow of gases in pipes at low pressures," J Appl Phys 17, 802–812 (1946)

[6] Weber, S, "Uber Deu Zusammenhang Zwischen Der Laminaven Stromung Dev Reinen Gase Durch Rohve Und Dem Selbstdiffusions-Koeffizieuten, Math -Fysiske Meddlelser, Bind 28, no 2, 138–272 (1954)

[7] Sparrow, E M and Jonsson, V K, "Free-molecule flow and convective energy transport in a tapered tube or conical nozzle," AIAA J 1, 1081–1087 (1963)

JUNE 1964 AIAA JOURNAL VOL 2, NO 6

Fuel Containment in the Gaseous-Core Nuclear Rocket by MHD-Driven Vortices

JACOB B ROMERO*
The Boeing Company, Seattle, Wash

A gaseous fission propulsion engine is considered in which an electromagnetic vortex is employed for fuel retention The pertinent continuity, momentum, energy, diffusion, and electromagnetic equations are derived for steady-state, laminar, two-dimensional flow and are solved for several cases Economical fuel retention is considered from the point of view of rocket performance and design Two basic design concepts are considered: a single critical chamber and multiple vortex tubes Engine thrust-to-weight ratios range from ten-thousandths for the single vortex designs to tenths for the multiple vortex designs Bypass flow systems are suggested as a means of obtaining performance improvement

Nomenclature

B_0 = uniform axial magnetic flux density, webers/m^2
B_z = axial magnetic flux density, webers/m^2
c_p = gas heat capacity, joules/kg/°K
D_{12} = diffusion coefficient of heavy gas in light gas, m^2/sec
E_r = radial electric field strength, newtons/coul
H = gas enthalpy, joules/mole
I = radial current, amp/m
j_r = radial current density, amp/m^2
k = gas thermal conductivity, joules/m/sec/ K
K = Boltzmann constant, joules/°K
L = length of vortex, m
m = mass of gas molecule, kg
m_T = fuel mass inside chamber, kg
m_c = critical mass, kg
N_{Pr} = Prandtl number
n_p = particle number density at r, number/m^3
N_{Re} = radial Reynolds number
N_{Sc} = Schmidt number
p = gas pressure, newtons/m^2
P = electric power loss, w/m
q = conduction heat transfer, joules/sec/m^3
Q_f = energy released per fission, joules
Q_v = nuclear heat addition, joules/m^3
r = radial distance (coordinate), m
r^+ = (r/r), dimensionless radial distance (coordinate)
R = universal gas constant, joules/kg/mole/°K
T = gas temperature, °K
U = potential drop across vortex, v
v_r = radial gas velocity, m/sec
v_t = tangential gas velocity, m/sec
w = flow rate, kg/sec/m
Z = axial distance (coordinate), m
σ_f = fission cross section, m^2
μ = gas viscosity, kg/sec/m
ω = angular velocity, rad/sec
ρ = gas density, kg/m^3
ρ^+ = ratio of fuel to propellant mass densities
σ = gas electrical conductivity, mho/m
θ = tangential coordinate
ϕ = neutron flux, number/sec/m^2
Φ = viscous heat dissipation, joules/m^3

Subscripts

1 = refers to species 1 or propellant
2 = refers to species 2 or fuel
m = refers to position where the tangential velocity has a maximum
i = refers to inner electrode outer radius
o = refers to outer electrode inner radius

Received July 23, 1963; revision received March 4, 1964 The assistance of J C Almond and D E Heard with the computer calculations is gratefully acknowledged Barbara Romero assisted in typing the rough manuscript Assistance in preparing and arranging the final manuscript and graphic art was rendered by G L Case, N E Evans, H T Martin, P C Canup, and H J Mosich of the Boeing Audio-Visual Support and Publishing Section

* Lead Engineer, Advanced Nuclear Group Member AIAA

Introduction

PERFORMANCE of solid-core nuclear propulsion engines is limited by low maximum operating temperatures imposed by structural materials in the solid core To overcome these temperature limitations, the gaseous-core nuclear propulsion engine has been suggested, in which both fuel and propellant are injected into the chamber itself, thereby avoiding major contact with structural surfaces and allowing higher temperature operation

Unfortunately, loss of fuel in the rocket exhaust poses an equally difficult problem The fuel loss is so great that, without some form of fuel retention, the gaseous-core engine is economically impractical In order to solve this problem, several fuel retention schemes have been proposed [1–7] This paper discusses a few of these schemes and describes one, the MHD-driven vortex, in considerable detail

In the MHD vortex, a uniform electric current flows between electrically insulated coaxial electrodes, and a magnetic field is applied axially A partially ionized gas flowing uniformly between outer and inner electrodes receives a tangential force, thereby forming a vortex High tangential velocities[8–11] that force the denser fuel to the chamber walls are im-